Pergamon

0964-1807(95)00078-X

Applied Superconductivity Vol. 3, No. 7–10, pp. 383–398, 1995
Published by Elsevier Science Ltd

0964-1087/95 $9.50 + 0.00

MULTILAYER MAGNETOMETERS BASED ON HIGH-T_c SQUIDS

F. LUDWIG†, E. DANTSKER, D. KOELLE‡, R. KLEINER, A. H. MIKLICH* and J. CLARKE

Department of Physics, University of California, Berkeley, CA 94720, U.S.A.

and

Materials Sciences Division, Lawrence Berkeley National Laboratory, Berkeley, CA 94720, U.S.A.

Abstract—Recent progress towards the development of a multilayer technology for the high transition temperature superconductor $YBa_2Cu_3O_{7-x}$ (YBCO) is described. Early YBCO–$SrTiO_3$–YBCO multilayers, fabricated with laser deposition and patterning of each layer, were plagued with excess magnetic flux noise at low frequencies. This noise was generated by the thermally activated hopping of flux vortices between pinning sites in the superconducting films. The progressive reduction in the level of this noise by improving the quality of the films is described. A key issue is the protection of the first YBCO film with a thin $SrTiO_3$ cap before patterning. This process, which currently produces the lowest level of 1/f noise, was used to fabricate a number of multilayer structures. A multiturn flux transformer coupled to a single-layer dc superconducting quantum interference device (SQUID) in a flip-chip arrangement achieved a magnetic field noise at 77 K of 8.5 fT $Hz^{-1/2}$ at 1 kHz and 27 fT $Hz^{-1/2}$ at 1 Hz; the pickup loop was 10 mm across. A monolithic 16-turn multiloop magnetometer with a diameter of 7 mm and operated at 77 K yielded 18 fT $Hz^{-1/2}$ at 1 kHz and 37 fT $Hz^{-1/2}$ at 1 Hz.

1. INTRODUCTION

The superconducting quantum interference device (SQUID) is a highly sensitive detector of magnetic flux. This sensitivity can be exploited for the measurement of any physical quantity that can be converted into magnetic flux, for example, magnetic field, magnetic field gradient, magnetic susceptibility and voltage [1]. Over the last several years, there has been a steady reduction in the noise of SQUIDs made of the high-T_c superconductor $YBa_2Cu_3O_{7-x}$ (YBCO) and operated at 77 K. Several groups have reported dc SQUIDs with a magnetic flux noise of a few $\mu\Phi_0 Hz^{-1/2}$, corresponding to noise energies of about 10^{-30} JHz^{-1}, at frequencies above the 1/f region [2–7]; typically, 1/f noise dominates at frequencies below a few Hz. Here, $\Phi_0 = h/2e$ is the flux quantum. The most sensitive devices involve grain boundary junctions, made on either $SrTiO_3$ bicrystal substrates [2,4,6,7] or step edges etched into a substrate by ion milling [3,5,8,9].

To make a sensitive magnetometer from a SQUID, one has to increase its effective area while keeping its inductance low. Figure 1 shows four high-T_c magnetometer designs, two involving single layers of YBCO (a, b) and two involving multilayers (c, d). The directly coupled magnetometer made by Koelle *et al.* [10] consists of a dc SQUID connected to a pickup loop patterned in the same YBCO film (Fig. 1a). Zhang *et al.* [11] increased the effective area of their rf SQUIDs by making washers of YBCO with large outer dimensions (Fig. 1b). Subsequently, both groups further reduced the magnetic field noise by inductively coupling their devices to a large single-turn flux transformer patterned in 50 and 40 mm diameter YBCO films, respectively. The noise with the directly coupled magnetometer was 31 fT $Hz^{-1/2}$ at 1 kHz, increasing to 39 ft $Hz^{-1/2}$ at 1 Hz [4], and with the rf SQUID 24 fT $Hz^{-1/2}$ at frequencies above about 1 Hz

† Present address: Physikalisch-Technische Bundesanstalt Berlin, Abbestr. 10–12, 10587 Berlin, Germany.
‡ Present address: Lehrstuhl für Experimentalphysik II, Universität Tübingen, 72076 Tübingen, Germany.
* Present address: Westinghouse STC, MS 401-3A13, 1310 Beulah Road, Pittsburgh, PA 15235-5098, U.S.A.

[12]. More recently, Cantor *et al.* [13] reported a directly coupled magnetometer fabricated on a 20 × 20 mm $SrTiO_3$ bicrystal, achieving a magnetic field noise of $S_B^{1/2}(1\text{ kHz}) = 14\text{ fT Hz}^{-1/2}$ and $S_B^{1/2}$ (1 Hz) = 26 fT $Hz^{-1/2}$. Although these noise levels are sufficiently low for a number of applications, the relatively large size of these devices may prevent one from achieving a reasonably dense array of devices, for example, for magnetocardiology. The large size of the pickup loops necessary to achieve such low field noise values arises from the inefficient flux transfer into the SQUID.

More efficient coupling schemes require multilayer structures. The usual way of enhancing the effective area of a SQUID is to couple the SQUID to a superconducting flux transformer [1], shown schematically in Fig. 1c. The transformer is a closed superconducting circuit consisting of a large pickup loop to sense the magnetic field and a much smaller, multiturn input coil to couple flux into the SQUID. To optimize the flux transfer into the SQUID, the inductance of the input coil is chosen to match that of the pickup loop. An alternative multilayer approach is the magnetometer (or fractional turn SQUID), shown schematically in Fig. 1d. The essential idea of this device, orginally proposed by Zimmerman [14], is to connect N pickup loops in parallel, thus decreasing the total inductance while maintaining a large effective area.

In designing and fabricating high-T_c mutilayer magnetometers, one should bear in mind two matters concerning noise. The first is the influence of thermal noise on the flux-to-voltage transfer function $V_\Phi = dV/d\Phi$ and magnetic flux noise $S_\Phi^{1/2}(f)$ of the SQUID. This issue is addressed briefly in Section 2, along with other design considerations. Second, although multiturn flux transformers made of YBCO have been reported by a number of groups, these multilayer structures can produce significant levels of low-frequency 1/f noise. This noise arises from the thermally activated motion of vortices in the YBCO films that tend to be of poorer quality in patterned multilayers than in single layers. For some applications, notably biomagnetism, low levels of magnetic field noise are required at frequencies down to 1 Hz or below. Our efforts to reduce the level of 1/f noise by progressively improving the fabrication process are described in Section 3. Section 4 describes the performance of our multiloop devices and of our magnetometers with multiturn flux transformers, either inductively coupled to a SQUID in a flip-chip configuration or integrated with the SQUID on the same chip. We conclude with a comparison of the different approaches and mention some remaining problems. Most of this work has been published previously in a series of short articles [15–19].

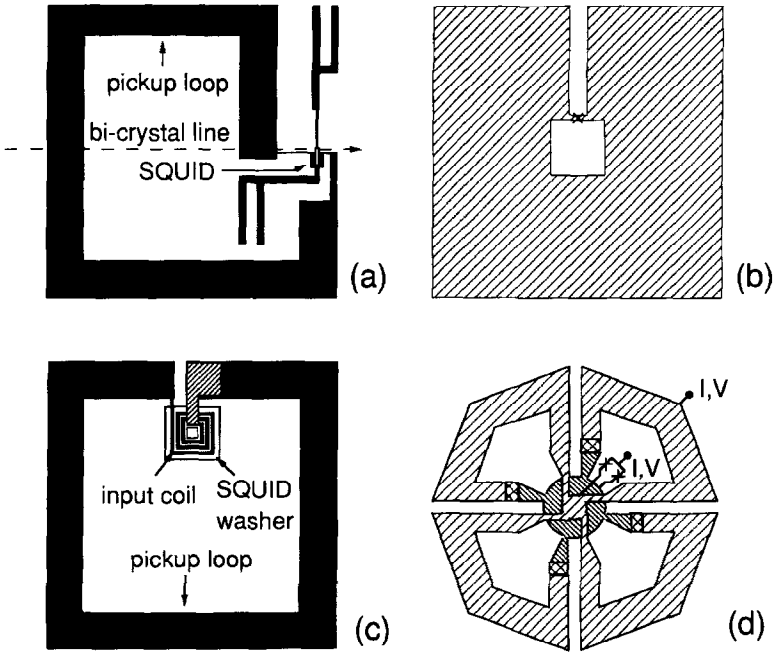

Fig. 1. Four magnetometer designs: (a) directly coupled magnetometer, (b) large-washer rf SQUID, (c) SQUID coupled to flux transformer, and (d) fractional turn SQUID.

2. DESIGN CONSIDERATIONS

To obtain a low magnetic field noise $S_B^{1/2}(f) = S_\Phi^{1/2}(f)/A_{eff}$, one should make the flux noise of the SQUID, $S_\Phi^{1/2}(f)$, small and the effective magnetometer area, A_{eff}, large. Here, $S_\Phi^{1/2}(f) = S_V^{1/2}(f)/V_\Phi$, where $S_V^{1/2}(f)$ is the voltage noise across the SQUID. Generally speaking, it is easier to make A_{eff} large if the SQUID inductance L is large; however, increasing L decreases V_Φ Thus, the choice of an appropriate value of L is a key issue.

Typical low-T_c SQUIDs for operation at 4.2 K have inductances L on the order of 100 pH and are designed with $\beta_L = 2LI_0/\Phi_0 \gtrsim 1$; I_0 is the critical current of each junction. These values lead to a noise parameter $\Gamma = 2\pi k_B T/I_0\Phi_0 \lesssim 0.02$. Under these conditions, the flux-to-voltage transfer coefficient is given approximately by $V_\Phi \approx 4I_0R/(1+\beta_L)\Phi_0$, where R is the shunt resistance of each junction [20]. For high-T_c SQUIDs at 77 K, however, Koelle *et al.* [10] observed that, for $L > 40$ pH, V_Φ decreased with increasing inductance more rapidly than the above formula predicts. In retrospect, the explanation is straightforward: when one designs a SQUID for operation at 77 K rather than 4.2 K, it is impracticable to reduce L by a factor of 20 to (say) 5 or 10 pH. Thus, if one retains $\beta_L \gtrsim 1$, the value of Γ at 77 K is appreciably higher than at 4.2 K. Careful stimulations with appropriate parameters [21–24] are in good agreement with the observed decrease in V_Φ with increasing L. The essential conclusion from this work is that L should generally be kept below 80 pH to avoid a drastic fall-off in V_Φ. We note that for $L = 80$ pH and $\beta_L = 1$, the corresponding value of I_0 is about 13 μA. The upper limit on the I_0R product for grain boundary junctions is about 200 μV, implying a corresponding resistance of about 15 Ω. In practice, it is not so easy to obtain such high resistance values without resorting to submicron lithography; however, Lee *et al.* [6] have reported bicrystal junctions with resistances of 10–20 Ω for a junction width of 2 μm.

To increase the effective area of a SQUID one conventionally couples it to a flux transformer (Fig. 1c). It is straightforward to show [1] that the effective magnetometer area is given by

$$A_{eff} = A_s + A_p \frac{M_i}{L_i + L_p}, \tag{1}$$

where A_s is the effective area of the base SQUID (including flux focusing effects [25]), $M_i = \alpha(LL_i)^{1/2}$ is the mutual inductance between the SQUID of inductance L and the input coil of inductance L_i, α is the coupling coefficient, and L_p and A_p are the inductance and area of the pickup loop. Assuming that α does not depend on L_i and L, the effective area is a maximum when $L_i = L_p$, yielding

$$A_{eff} = \frac{\alpha}{2}\sqrt{L}\frac{A_p}{\sqrt{L_p}}, \tag{2}$$

where we have neglected A_s which is usually small. To maximize A_{eff}, we must maximize $A_p/\sqrt{L_p}$. One can optimize the ratio $A_p/\sqrt{L_p}$, by using $A_p = dD$ [25] for the effective area of the pickup loop and

$$L_p = \frac{1.86}{\pi}\mu_0\left(\frac{D+d}{2}\right)\left[\ln\frac{D+d}{D-d} + 0.42\right] \tag{3}$$

for its inductance. Here D and d are the outer and inner dimensions of the square pickup loop. Equation (3) was obtained by Drung [26], who fitted the inductance calculated by Jaycox and Ketchen for a square washer (Fig. 1 in Ref. [27]), thus covering a large range of linewidths. For a pickup loop with an outer length of $D = 10$ mm we find an optimum linewidth of about 1 mm. This is in contrast to the directly coupled magnetometer where the ratio A_p/L_p has to be maximized, yielding an optimum design which is a washer [6, 13].

Furthermore, to obtain the largest possible effective area α should be as high as possible. We measured α for different SQUID designs [18], either coupled to the same 16-turn flux transformer in a flip-chip arrangement or integrated with a flux transformer on the same chip. The SQUID configurations, B, C, A/C and A/A are shown schematically in Fig. 2. We found that α varies with the SQUID design, being higher for type A/A and A/C ($\alpha \gtrsim 0.5$ even for flip-chip magnetometers) than for type B and C. We also found that the screening of the input coil

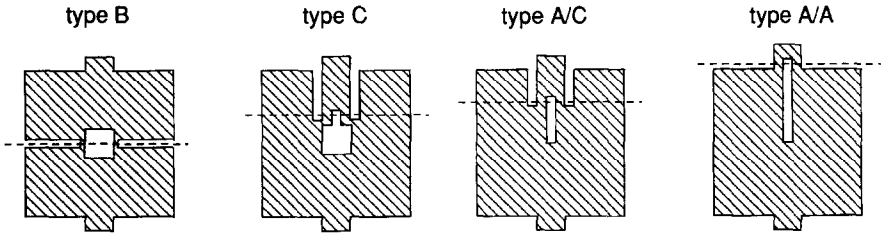

Fig. 2. Four types of dc SQUID. Dashed line indicates grain boundary.

inductance by the SQUID washer decreases appreciably for input coil thicknesses below about 120 nm, thus increasing L_i and resulting in a lower effective coupling coefficient [16]. In addition, in the integrated devices, the type A/A SQUID has the advantage that the junctions are located outside the washer, so that the narrow lines of the input coil do not cross the bicrystal boundary. Although A_{eff} increases with increasing SQUID inductance L, larger values of L do not necessarily produce lower magnetic field noise. Using equation (2) for the effective magnetometer area, one finds $S_B(L) \propto S_\Phi(L)/L$. Thus, minimizing S_B with respect to L is equivalent to minimizing the noise energy $S_\Phi/2L$.

An alternative approach is the multiloop magnetometer (fractional turn SQUID) shown in Fig. 1d. Each of the N pickup loops makes contact to both superconducting films in the patterned trilayer in the center of the device. The two junctions in series connect the upper and lower superconducting films. The effective inductance is given by [28]

$$L_{\text{eff}} = \frac{L_p}{N^2} + \frac{L_s}{N} + L_j, \tag{4}$$

and the effective area by

$$A_{\text{eff}} = \frac{A_p}{N} - A_s. \tag{5}$$

Here, L_p and A_p are the inductance and area of the large, outer loop, L_s and A_s are the average inductance and area of one spoke of the "cartwheel," L_j is the inductance of the connections from the pickup loops to the junctions, and N is the number of loops that are connected in parallel. Using the flux noise simulations of Enpuku *et al.* [21], Drung *et al.* [28] calculated that the magnetic field noise has a broad minimum for $N = 15$–20, assuming $T = 77$ K and a device diameter of 7 mm. This optimized value of N is roughly a factor of two higher than that for $T = 4.2$ K. A detailed discussion of the design optimization is given in ref. [28].

3. FABRICATION

Multiturn flux transformers [Fig. 1c] and multiloop magentometers (Fig. 1d) require two superconducting layers separated by an insulating layer. One must be able to connect the two superconductors through windows (vias) in the insulator. For YBCO films, $SrTiO_3$ is usually chosen as the insulator because of the excellent lattice match. In their early development of high-T_c interconnects, Kingston *et al.* [29] used shadow masks to define the geometry of the lower YBCO film and the insulating $SrTiO_3$ film, and photolithography to pattern the upper YBCO film. This technology was subsequently used by Roas *et al.* [30]. The advantage of this process is that the surfaces of the films are never exposed to photoresist and etching chemicals; in fact, the entire process could in principle be performed *in situ*. Furthermore, the use of shadow masks yields patterned structures with smooth, gently sloping edge profiles, allowing the crystalline growth of subsequent films over the edge. The obvious disadvantage is that shadow masks cannot be used for more complicated circuitry or to define micrometer-scale geometries. Thus, it was essential to develop processes in which all layers are patterned photolithographically. Such procedures have been developed by a number of groups [31–37]; an overview is given in Ref. [38].

3.1 Early multilayer process

In our early photolithographic process [31,35], the first YBCO film, typically 300 nm thick and deposited on a (100) MgO substrate, was patterned by wet-etching in 0.05–0.1% nitric acid. The resist was stripped and the sample was immersed in a 1% solution of Br in methanol to etch the YBCO surface. Then a 400 nm-thick $SrTiO_3$ layer was deposited. To open a window in the $SrTiO_3$, an Ar ion beam at an angle of incidence of 60° was used to produce a via with beveled edges. To ensure complete removal of the $SrTiO_3$ and provide in-plane contact between the upper and lower YBCO films, we attempted to ion mill roughly 100 nm into the lower YBCO film. After stripping the resist, we deposited a second YBCO film, typically 400 nm thick, and acid-etched it. All the films were deposited using a pulsed KrF excimer laser.

With this interconnect technology, we successfully fabricated multiturn flux transformers operating at 77 K [35,39]. Figure 3 shows $S_B^{1/2}(f)$ and $S_\Phi(f)$ for a magnetometer consisting of a 81 mm^2 pickup loop and a five-turn input coil coupled in a flip-chip configuration to a sensitive 500 μm washer SQUID with bicrystal junctions. In this arrangement, the SQUID and the flux transformers are made on separate substrates and clamped together to form a magnetometer. The SQUID, immersed in liquid nitrogen and enclosed in a 40 mm diameter Conetic shield, was operated in a flux-locked loop with a 100 kHz flux modulation scheme and bias reversal [40] to reduce 1/f noise due to critical current fluctuations. Unless noted otherwise, all data presented in this paper were obtained with this double modulation scheme. The dewar was surrounded with a triple mu-metal shield. The flux noise power of the bare SQUID is indicated schematically by the dashed line. The flux transformer increased the effective area of the bare SQUID by a factor of about 80 yielding a white noise of approximately 36 fT $Hz^{-1/2}$. However, at frequencies below a few kHz the noise power scaled as 1/f, and was caused by the motion of vortices in the YBCO films of the transformer. The high level of magnetic field noise at 1 Hz (1.7 pT $Hz^{-1/2}$) stressed the need to improve our multilayer technology to obtain lower levels of flux noise.

3.2 Single YBCO and in situ *YBCO–$SrTiO_3$–YBCO trilayer films*

Since the 1/f noise of YBCO films decreases dramatically as their crystalline quality is improved [41,42], we made systematic efforts to improve the quality of both our YBCO single-layer and YBCO–$SrTiO_3$–YBCO multilayer films. To improve the lattice match to YBCO and obtain a better crystalline growth, we replaced the MgO substrates with (100) $SrTiO_3$ substrates, buffered with about 10 nm of $SrTiO_3$. We also improved the film quality by reducing the deposition rate from 0.2 nm/pulse [35] to 0.06–0.07 nm/pulse. We grew these multilayer films *in situ*, that is, without breaking the vacuum between depositions. For a single YBCO film, we

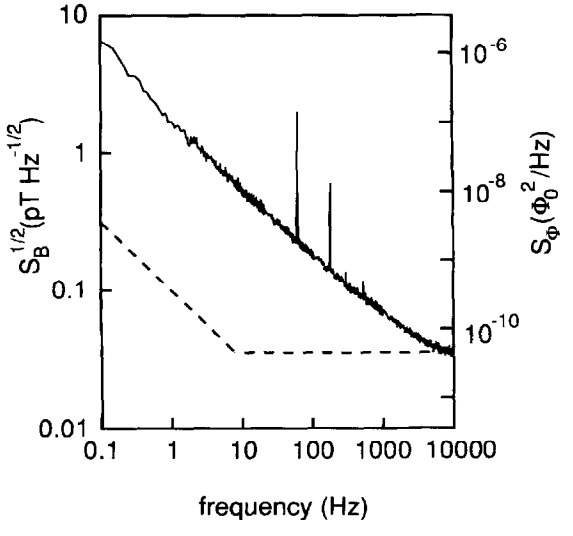

Fig. 3. Magnetic field noise $S_B^{1/2}(f)$ and flux noise power $S_\Phi(f)$ vs frequency for early transformer [39] coupled to 40 pH SQUID with bicrystal junctions. Dashed line indicates flux noise power of bare SQUID.

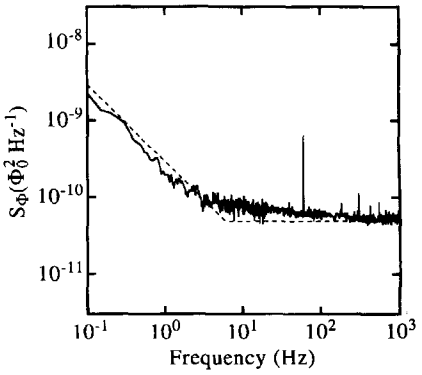

Fig. 4. Flux noise $S_\Phi^{1/2}(f)$ vs frequency for *in situ* YBCO–$SrTiO_3$–YBCO trilayer. Dashed line indicates flux noise of bare SQUID.

typically obtain transition temperatures $T_c = (89–90)$ K and critical current densities j_c (77 K) = (3–5) × 10^6 Acm^{-2}. For *in situ* trilayers with a lower YBCO film thickness of 120 nm and a $SrTiO_3$ film of 250 nm, we measured $T_c = (88–89)$ K and j_c (77 K) = (2–3) × 10^6 Acm^{-2} for the upper, 250 nm-thick YBCO film.

We also performed X-ray diffraction measurements, which indicated a high degree of crystalline quality: the half-width at full maximum of the rocking curve of the (005) peak was below 0.3°.

To investigate the flux noise of trilayer films, we coupled them to a high-T_c dc SQUID in a flip-chip arrangement and measured the noise at 77 K. Figure 4 shows that the presence of the trilayer did not increase the 1/f flux noise of the SQUID over that of the bare SQUID, $S_\Phi^{1/2}(1\text{ Hz}) = 15\ \mu\Phi_0\ \text{Hz}^{-1/2}$. By comparison, the flux noise of the upper YBCO film of a trilayer fabricated with film thicknesses typical for the earlier process (300 nm for the lower YBCO film, 400 nm for the $SrTiO_3$ and upper YBCO films), was always above 100 $\mu\Phi_0\ \text{Hz}^{-1/2}$ at 1 Hz.

3.3 Patterned YBCO–$SrTiO_3$–YBCO trilayers

The noise of the *in situ* trilayers is in principle low enough to enable one to make multiturn flux transformers which do not couple excess low-frequency flux noise into the SQUID. However, each film in the multilayer structure has to be patterned separately, that is, it must be exposed to photolithographic processing. Furthermore, a patterning process is needed that produces edges over which subsequent layers grow with a high degree of crystallinity. To study the properties of the various transformer components, we fabricated test structures to enable us to make independent electrical measurements of the lower and upper YBCO films, the crossover where the upper YBCO film passes over the lower film, the via connecting them through the insulating layer, and the insulation itself.

Following our earlier process, we wet etched the lower YBCO film in 0.05% HNO_3 and etched it for 5–6 s in a 1% solution of Br in methanol. We then deposited the $SrTiO_3$ insulating layer and cut a via with Ar ion milling at a 60° angle of incidence. In contrast to the former process, the ion milling also removed all of the lower YBCO film in the window area, leaving only a beveled edge to make contact to the upper YBCO film, which was also wet etched.

With the film thicknesses quoted above, we found that j_c (77 K) for the upper YBCO film remained at (2–3) × 10^6 Acm^{-2} even where it crossed the edges of the lower YBCO strip. This was a substantial improvement over the earlier crossovers using thicker YBCO and $SrTiO_3$ films. The reason is made clear in Fig. 5, which shows scanning electron microscope (SEM) images of edges of YBCO films patterned with wet etching (a) without Br etching and (b) after a 10 s Br etch. We see in (a) that the edge of a 300 nm film is almost perpendicular to the substrate. For a 200 nm film (b), the Br etch rounds the upper part of the edge; for thicknesses below 150 nm, the entire edge tends to become bevelled. Thus, the Br etch can produce reasonably smooth edges for thinner films, but steep edges remain for thicker films. In the latter case, subsequent films presumably grow with disorder and grain boundaries, and thus have relatively low critical currents. We note that the surfaces in Fig. 5 have been roughened by the etching process.

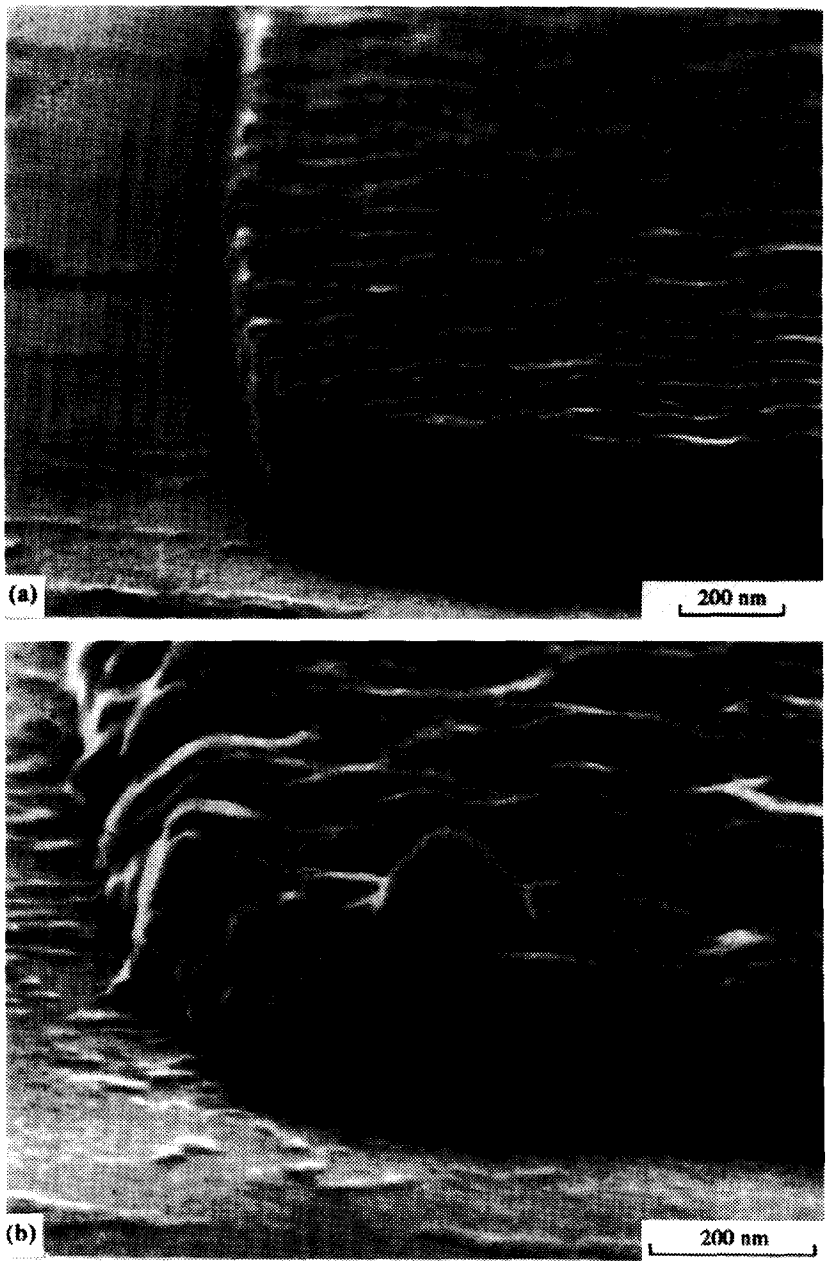

Fig. 5. SEM image of (a) 300 nm thick YBCO film etched in 0.05% HNO_3 with no Br etch, and (b) 200 nm thick YBCO film etched in 0.05% NNO_3 with 10 s etch in 1% Br in methanol.

The vias, on the other hand, were made by Ar ion milling with a 60° angle of incidence, producing a smooth beveled edge with a slope of 7–10°, thus allowing the relatively smooth growth of the upper YBCO film [15]. For a 30 μm wide via contact and a lower YBCO film thickness of 100 nm the critical current I_c (77 K) was typically 15 mA, corresponding to $j_c \leqq 5 \times 10^5$ Acm^{-2}. Although this value is almost one order of magnitude lower than for single films, it is adequate for flux transformers. The resistivity of the $SrTiO_3$, measured between the upper and lower YBCO films over an area of 20 × 100 μm^2, was typically 10^8 Ωcm or higher at 77 K.

We used this improved interconnect technology to fabricate a series of flux transformers with pickup loop areas of either 68 or 81 mm^2, and mostly with 16-turn input coils. Both the input coil and the pickup loops were patterned in the lower YBCO film, with linewidths of 7 μm and 1 mm,

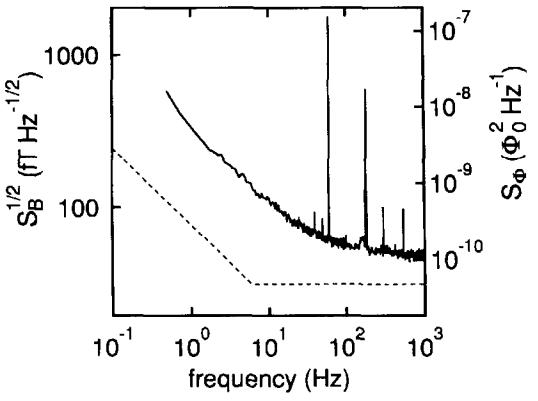

Fig. 6. Magnetic field noise $S_B^{1/2}(f)$ and flux noise power $S_\Phi(f)$ vs frequency for 16-turn flux transformer coupled to 40 pH SQUID. Dashed line indicates flux noise power of bare SQUID.

respectively. Out of eight flux transformers, seven operated at 77 K, indicating that the fabrication process was fairly reproducible. We coupled each transformer in turn to a dc SQUID with an outer dimension of 500 μm in a flip-chip arrangement. Figure 6 shows $S_B^{1/2}(f)$ and $S_\Phi(f)$ vs frequency for the best magnetometer. The magnetic field gain was 70, yielding $S_B^{1/2}$(1 kHz)=30 fT Hz$^{-1/2}$ and $S_B^{1/2}(1\text{ Hz}) = 340$ fT Hz$^{-1/2}$. The latter value represented a factor of five improvement over the best flip-chip magnetometer fabricated with the old process. Nevertheless, the rms flux noise at 1 Hz was still a factor of five above that of the bare SQUID, implying that noise from the flux transformer still dominated at low frequencies.

To investigate the origin of the low-frequency flux noise, we used the same high-T_c SQUID in a flip-chip configuration to measure the flux noise produced by single, bilayer and trilayer test regions patterned on the same chip as the flux transformers. Furthermore, in some cases, we opened the pickup loop of the transformer and re-measured the flux noise to distinguish between direct and indirect noise contributions [42]. We found that the 1/f noise of the *ex situ* trilayers was usually the highest, although we could not rule out the possibility that the YBCO film at the edges of the via and crossover also contributed to the noise. On the other hand, as before, the flux noise of trilayers that had been fabricated *in situ*, that is, without breaking the vacuum between depositions, did not measurably increase the flux noise of the high-T_c SQUID (see Fig. 4). Thus, the enhanced low-frequency flux noise of the trilayers in the flux transformer structures was related to the nature of the *ex situ* process.

To characterize the *ex situ* process, we studied the growth of $SrTiO_3$ on a YBCO film that had been subjected to the usual processing, but was not patterned: after depositing a 120 nm-thick YBCO film on a (100) $SrTiO_3$ substrate buffered with a 10 nm-thick $SrTiO_3$ layer, we spun on photoresist, developed and removed it with acetone and then etched the sample surface for about 5 s in 1% Br in methanol. We then deposited a 250 nm-thick $SrTiO_3$ film. The surface of the bilayer imaged with an atomic force microscope (AFM) is shown in Fig. 7a. In addition to several large (100–150 nm) particles, there are many plate-like particles, typically 200 nm on a side and 20 to 25 nm high, on a relatively smooth surface with a roughness of a few nm.

For comparison, Fig. 7b shows the surface of a bilayer in which we capped the lower YBCO film with an 15 nm-thick *in situ* $SrTiO_3$ film before exposing it to photoresist. As before, we deposited a 230 nm-thick $SrTiO_3$ film after removing the photoresist. We see that the particles evident in Fig. 7a are no longer present, and the surface roughness is 2–3 nm. Thus, the poor growth of the $SrTiO_3$ film, which determines the structure of the upper YBCO film and consequently its flux noise, appears to arise from damage induced on the surface of the lower YBCO film by photoresist and Br etching.

Subsequently, we modified our fabrication process by introducing the capping step; several other groups [37,43–45] use a similar process. After depositing the lower YBCO film, we cap it with a 15 nm-thick *in situ* $SrTiO_3$ film. The capped lower YBCO film is patterned by standard

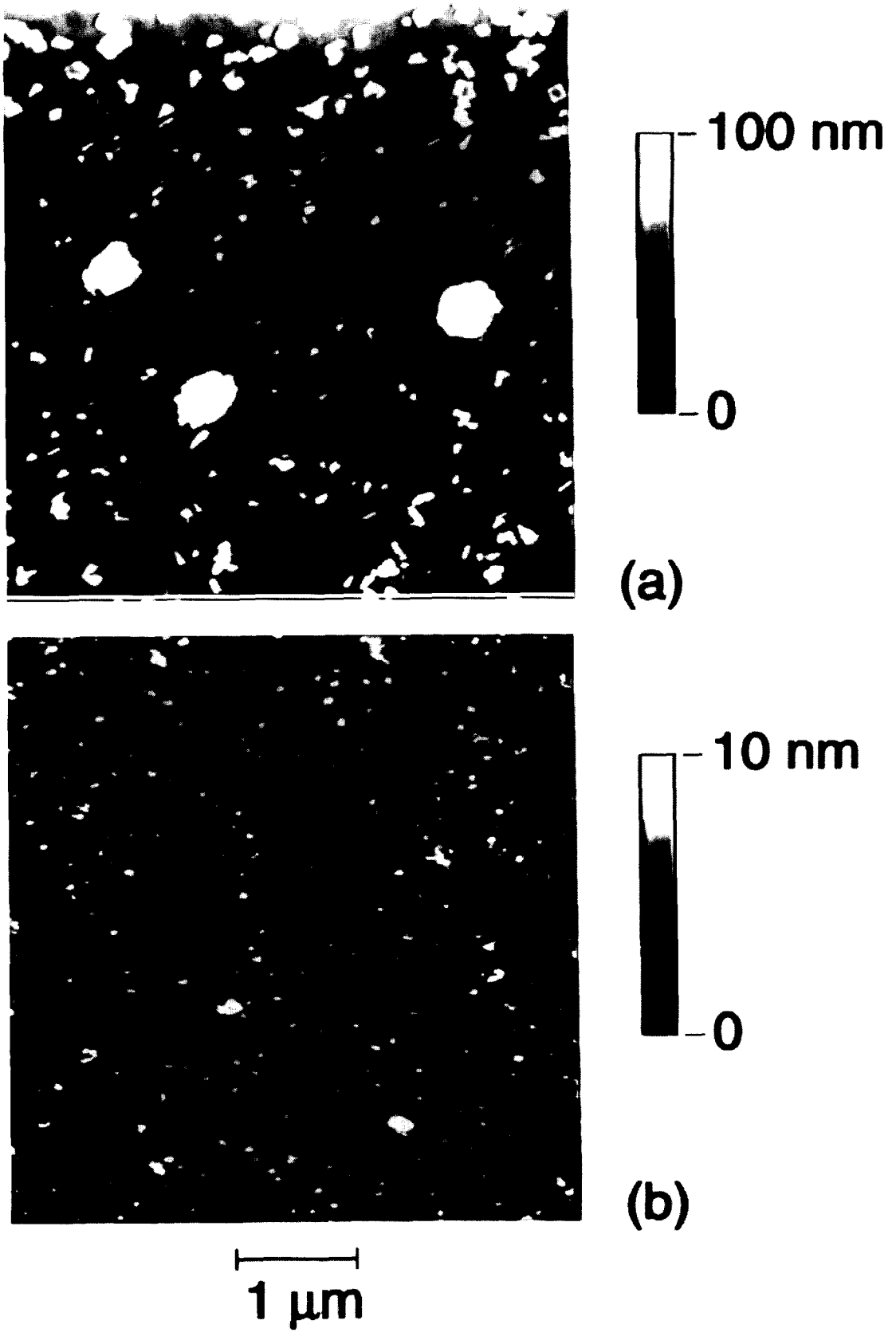

Fig. 7. AFM image of $SrTiO_3$ deposited on YBCO film (a) without and (b) with an *in situ* $SrTiO_3$ cap layer. Note 10 × increase in vertical magnification in (b).

Table 1. Deposition parameters for current multilayer process

Layer	Thickness (nm)	Deposition temperature (°C)	Oxygen pressure (mtorr)	T_c (K)	j_c(77 K) (10^6 Acm^{-2})
Lower YBCO	120–150	810	210	85	1–2
$SrTiO_3$ cap	15	760	150	—	—
$SrTiO_3$ insulator	230	760	150	—	—
Upper YBCO	250	790	210	89	3
Contact Ag	50	≈ 20	$< 10^{-3}$	—	—

photolithography and Ar ion milling. To bevel the edges of the film, we bake the photoresist after developing it for 10 min at 120°C to round the edges, and ion mill at a 60° or 45° angle of incidence while the substrate rotates. This procedure results in a smooth and gently beveled edge with an angle less than 20° [37]. After patterning the film, we strip the photoresist and deposit a 230 nm-thick $SrTiO_3$ film, which is patterned as described above. Finally, the upper YBCO film is deposited and patterned by Ar ion milling. In the case of integrated magnetometers, to provide electrical contacts we evaporate a 50 nm-thick Ag film immediately after the deposition of the upper YBCO film. In some cases, the Ag is deposited through a shadow mask so that no separate patterning step for the Ag layer is necessary. The deposition parameters for the various layers are listed in Table 1 together with measured transition temperatures T_c and critical current densities j_c (77 K) of the YBCO films.

Crossovers fabricated with the process described above have typical critical current densities of j_c (77 K) $= 3 \times 10^6$ Acm^{-2}; this value is similar to that in crossovers made without capping the lower YBCO films. For the patterned lower YBCO film we measured $T_c \approx 85$ K and j_c (77 K) $= (1\text{–}2) \times 10^6$ Acm^{-2}. In our prior process a 20 min cooldown from 780 to 450°C in 0.8 atm of O_2 was sufficient to oxygenate the lower YBCO film fully after it had been covered with a 250 nm-thick $SrTiO_3$ film. In contrast, the high crystalline quality of the $SrTiO_3$ insulator with the capping process inhibits oxygen diffusion into the lower YBCO film. With the same annealing process following the deposition of a 230 nm-thick $SrTiO_3$ film over a capped YBCO film, we found $T_c \sim 40$ K. To re-oxygenate the lower YBCO film, we introduced longer annealing steps in which we cool the sample to 500°C over a period of 30 min in 0.8 atm O_2 and maintain this temperature for 30 min and 3 h after the deposition of the $SrTiO_3$ capping layer and insulator, respectively. However, we never succeeded in fully recovering the parameters we routinely obtained for a bare YBCO film, namely $T_c = 89$ K and j_c (77 K) $= (3\text{–}5) \times 10^6$ Acm^{-2}. The same problem of oxygen deficiency has been reported by other groups; an alternative way of re-oxygenating a YBCO film covered with a high-quality insulator is to anneal it in an O_2 plasma [45].

We attempted to use X-ray diffraction to quantify the improvement in the growth of the upper YBCO film due to the capping process. We examined both single YBCO films and trilayers of two flux transformers previously characterized by flux noise measurements, one fabricated with the capping procedure and the other without. Measuring θ–2θ scans, rocking curves and φ scans, we could discern no significant differences in the crystallographic quality of the YBCO films in capped and uncapped trilayers. For example, the rocking curves for the YBCO (005) peaks had a full width at half-maximum of 0.2° for the lower YBCO film of both samples, and about 30% higher for both trilayers.

The fact that the X-ray data of both samples are indistinguishable is consistent with the excellent electrical properties which were measured on samples fabricated with the earlier, uncapped process. Most of the upper YBCO film is of excellent quality in both cases, and there is probably only a relatively small fraction of poor quality material for samples fabricated with the uncapped process. These regions, which may be related to the plate-like features on the $SrTiO_3$ surface (Fig. 7a), do not significantly influence X-ray data and critical current densities. On the other hand, they are presumably responsible for the higher $1/f$ flux noise in the upper YBCO film of uncapped trilayers.

4. RESULTS

Using the capping process described above, we fabricated multiturn flux transformers for flip-chip magnetometers, integrated magnetometers (SQUID and flux transformer integrated on the same chip) and multiloop magnetometers.

4.1 Flip-chip multiturn magnetometers

To make flip-chip magnetometers, we fabricated flux transformers with 16-turn input coils on 12 × 12 mm^2 (100) $SrTiO_3$ substrates. The substrates were polished on both sides enabling us to see through them while aligning the input coil with the SQUID. In most cases, the pickup loop and input coil were patterned in the lower YBCO film. The pickup loop was 10 mm on a side and had a width of 1 mm, giving a pickup loop area of about 80 mm^2. The input coil lines were 10 μm wide with a pitch of 14 μm. The crossovers and crossunders were 50 μm wide.

To enable us to select SQUIDs with low noise, we patterned 12 of them, six type A/A and six type A/C, in a 250 nm-thick, YBCO film deposited at Conductus on a $SrTiO_3$ bicrystal with a 24° misorientation angle. Each SQUID had an outer dimension of 500 μm, a slit width of 4 μm and junction widths between 1 and 3 μm. The resistance R per junction ranged from 2.4 to 8.6 Ω. The SQUID parameters are listed in Table 2; we selected the SQUID of each type with the largest peak-to-peak modulation voltage V_{pp}. To assemble the magnetometer, we carefully aligned the input coil of the transformer over the SQUID and clamped both chips together with a 3 μm-thick mylar sheet between them. The thickness of the mylar foil represents a lower limit for the SQUID-input coil separation; the actual spacing is presumably somewhat larger (5–10 μm).

The magnetic field noise achieved with the best flux transformer coupled to each SQUID is shown in Fig. 8. In contrast to our previous noise measurements, the magnetomer was enclosed in a superconducting shield. The shield consists of a 125 mm long yttria-stabilized zirconia tube with an inner dimension of 25 mm, coated on both sides with sintered YBCO [46]. We had previously noted that the white flux noise of the SQUID coupled to a flux transformer was increased over that of the bare SQUID (for example, Fig. 4 in Ref. [15] and Fig. 2a in Ref. [16]), suggesting that Nyquist noise from the Conetic shield may have limited the performance. When we replaced the Conetic shield with the superconducting shield, the white flux noise of the magnetometer was reduced to that of the bare SQUID [17,18]. In addition, the low-frequency

Table 2. Average junction resistance R, estimated inductance L, peak-to-peak modulation voltage V_{pp}, and effective area A_s of the bare SQUID; inductance L^c, and peak-to-peak modulation voltage V_{pp}^c of coupled SQUID; and effective area A_{eff} of magnetometer

SQUID	R (Ω)	L (pH)	V_{pp} (μV)	A_s (mm^2)	L^c (pH)	V_{pp}^c(μV)	A_{eff} (mm^2)
A/C	5.8	40	66	0.011	30	90	0.68
A/A	8.6	70	55	0.024	30	108	1.2

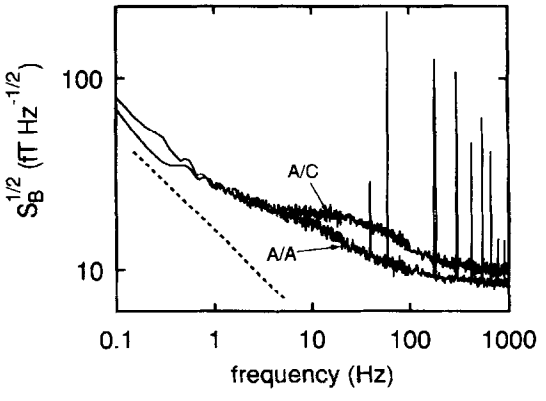

Fig. 8. Magnetic field noise $S_B^{1/2}(f)$ vs frequency of best A/C and A/A SQUID coupled to same flux transformer. Dashed line indicates $S_B^{1/2} \propto 1/f^{1/2}$.

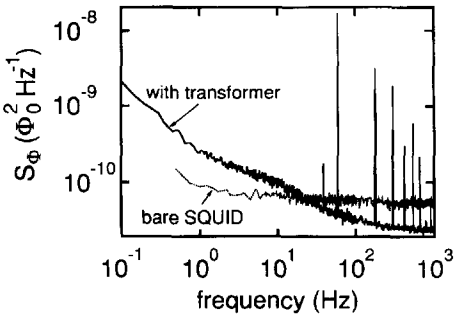

Fig. 9. Flux noise $S_\Phi^{1/2}(f)$ vs frequency for a bare A/A SQUId and the same SQUID coupled to a flux transformer.

(<10 Hz) noise and drift were reduced. All noise data reported in the following were obtained with the magnetometers mounted in the YBCO tube.

The magnetic field noise at 1 Hz is identical for both SQUIDs, 27 fT $Hz^{-1/2}$, suggesting that the low-frequency noise of the magnetometer is dominated by the "indirect noise" contribution of the flux transformer [42]; in this process the vortex motion induces a low-frequency noise current in the transformer which induces a flux in the SQUID. Alternatively, the noise could be environmental, for example, generated by the YBCO tube. At 1 kHz, where the noise is white, we measured 9.5 fT $Hz^{-1/2}$ and 8.5 fT $Hz^{-1/2}$ for the A/C and A/A devices, respectively. At frequencies above 1 Hz, the rms noise falls off more slowly than $1/\sqrt{f}$, and appears to have a contribution from a random telegraph signal.

In Fig. 9, the magnetic flux noise of the type A/A SQUID with and without a transformer is shown. We see that the flux noise at 1 kHz is reduced from 7.3 $\mu\Phi_0$ $Hz^{-1/2}$ to 4.9 $\mu\Phi_0$ $Hz^{-1/2}$ by the addition of the transformer. This reduction results from an increase in the peak-to-peak modulation voltage (Table 2), which, in turn, arises from the lowering of the SQUID inductance by the screening effect of the crossover in the flux transformer. For the type A/A SQUID, the crossover covers about 90% of the length of the slit in the SQUID washer; from simulations we estimate that the SQUID inductance is reduced from 70 to 30 pH.

4.2 Integrated multiturn magnetometers

We have investigated integrated magnetometers in which the transformer and the SQUID are deposited on the same substrate. Similar devices have been made by other groups [33,47–49]. We fabricated 10 integrated magnetomers, with a variety of SQUID designs and numbers of turns on the input coils [18], on each of two 10 × 10 mm^2 $SrTiO_3$ bicrystals. We used the SQUID washer as either a crossunder or crossover for the flux transformer, so that only two superconducting layers were necessary [47]. To accommodate 10 magnetometers on a chip, the pickup loops were necessarily small, either 1.8 mm^2 or 3.2 mm^2, so that the expected magnetic field sensitivity was relatively poor.

We measured the flux noise of the two best type A/A integrated magnetometers, one with an estimated inductance of 35 pH and an 8-turn input coil and the other with an inductance of 60 pH and a 12-turn input coil†. The flux noise of the latter was 19 $\mu\Phi_0$ $Hz^{-1/2}$ at 1 kHz and 25 $\mu\Phi_0$ $Hz^{-1/2}$ at 1 Hz. The rms white flux noise of this device was about a factor of two higher than the values we usually obtained for single layer SQUIDs with the same inductance although the asymptotic resistance per junction, $R = 1.5\ \Omega$, is a typical value. However, the noise-rounded critical current per junction was only 25 μA, yielding an I_0R product of roughly 50 μV, a factor of about three less than the values typically obtained for bicrystal junctions in single-layer SQUIDs. Furthermore, the V–Φ patterns for most of the integrated devices exhibited pronounced resonances, as had been observed by other groups [48,49]. These resonances degrade the SQUID performance; in future designs, they could be damped with a resistor shunting the two junctions

† In Ref. [18] we quoted SQUID inductances of 40 and 80 pH, respectively, estimating them using 0.4 pH/μm for the inductance of a slit in a wide superconductor [50]. Experimental results from Grundler *et al.* [51] obtained on directly coupled YBCO SQUIDs suggest that a value of about 0.3 pH/μm is more realistic.

[52]. If this particular device had been equipped with a 9-mm pickup loop, the magnetic field noise at 1 kHz would have been about 40 fT $Hz^{-1/2}$. This value is considerably poorer than that obtained with our best flip-chip devices, and is due entirely to the fact that the SQUID parameters were less than optimal. The most sensitive monolithic magnetometer involving a high-T_c SQUID with a multiturn flux transformer was fabricated on a 10 × 10 mm^2 substrate by Dössel *et al.* [53], and had a magnetic field noise of 39 fT $Hz^{-1/2}$ at 1 kHz. To increase the yield, they incorporated two SQUIDs, subsequently disconnecting the poorer one.

4.3 Multiloop magnetometers

For our high-T_c multiloop magnetometer we chose 16 parallel pickup loops with an outer diameter of 7 mm [18,28]. Using the values $N=16$, $L_p=12.2$ nH, $A_p=34.5$ mm^2, $L_s=1.17$ nH, $A_s=0.39$ mm^2, and $L_j=24$ pH, from equations (4) and (5) we obtain $L_{eff}=145$ pH and $A_{eff}=1.77$ mm^2. We fabricated and tested two such multiloop magnetometers on $SrTiO_3$ bicrystal substrates, in the configuration shown in Fig. 10. The two bicrystal junctions were patterned in the lower YBCO film and had a nominal width of 2.5 μm. The major portion of the 16 pickup loops was patterned in the upper YBCO film. In contrast to the integrated magnetometers where we evaporated the Ag contacts through shadow masks, we covered the whole sample with a 50 nm-thick Ag layer immediately after the deposition of the upper YBCO film, and subsequently patterned it.

For the better of the two devices we measured $R=10$ Ω and $I_c=4.3$ μA. Numerical simulations [18] indicated that the noise-free critical current per junction I_0 was about 13 μA, corresponding to $\beta_L \approx 1.8$; this value is close to optimum. The simulations yielded a peak-to-peak modulation voltage of $V_{pp} \approx 17$ μV, in quite good agreement with the measured value of 20 μV.

The magnetic field noise and the flux noise power of the device measured with static bias and bias reversal are shown in Fig. 11. The noise is 18 fT $Hz^{-1/2}$ at 1 kHz and 37 fT $Hz^{-1/2}$ at 1 Hz. Without bias reversal the magnetic field noise at 1 Hz increased to 105 fT $Hz^{-1/2}$.

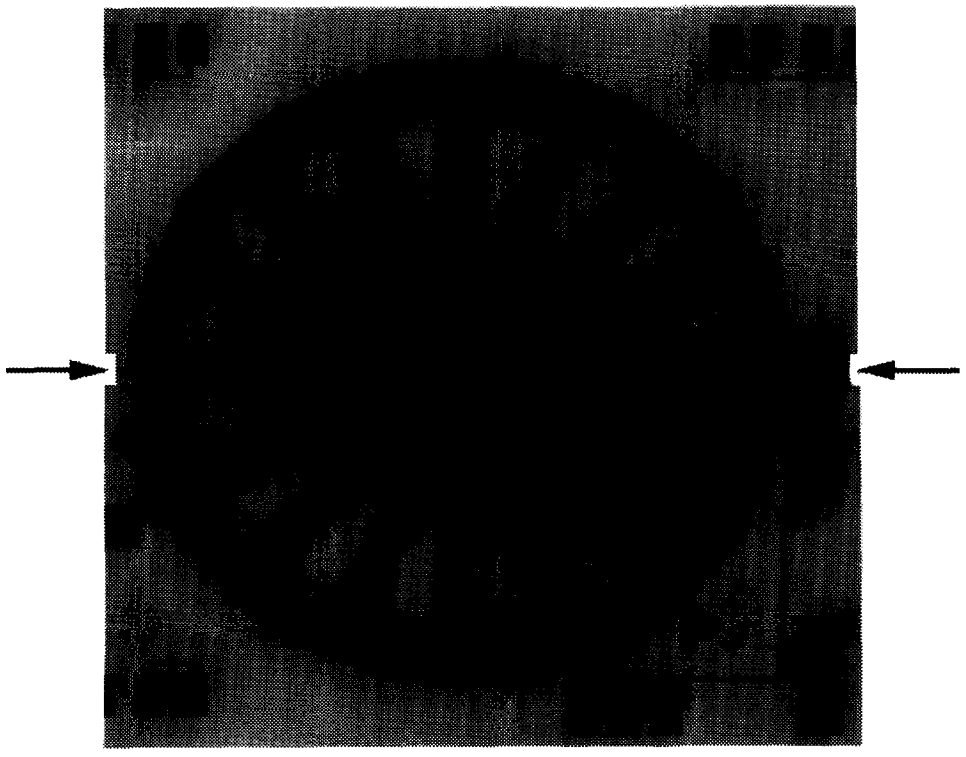

Fig. 10. Photograph of multiloop magnetometer, 7.2 mm in diameter. Arrows indicate grain boundary.

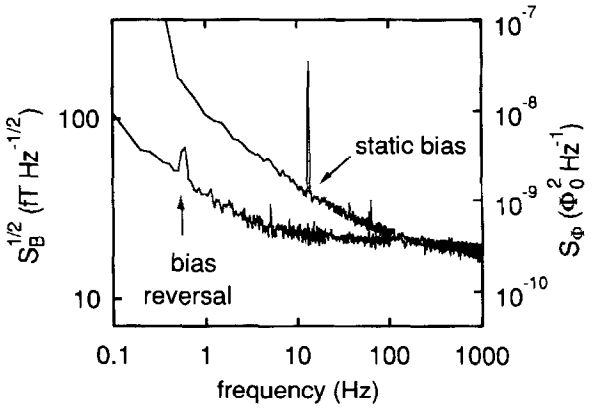

Fig. 11. Magnetic field noise $S_B^{1/2}(f)$ and flux noise power $S_\Phi(f)$ vs frequency for multiloop magnetometer measured with static bias and bias reversal, respectively.

5. CONCLUDING REMARKS

The magnetic field noise data presented in Section 4 demonstrate the progress that has been made towards the fabrication of YBCO multilayers with low $1/f$ noise. The currently available film quality and patterning techniques allow one to fabricate multilayer magnetometers with a magnetic field noise below 40 fT Hz$^{-1/2}$ down to 1 Hz. In this paper we have focused on our own work, but there are several groups with similar processes and comparable results [54].

Although various groups have reported the successful fabrication of integrated magnetometers, either as flux transformer coupled SQUIDs or as multiloop magnetometers, to date, the lowest magnetic field noise for a 10×10 mm^2 device has been achieved with a flip-chip magnetometer. The main advantage is that it allows one to select the lowest noise SQUID from a number made on the same substrate, giving a high yield of magnetometers with low noise. On the other hand, an integrated technology requires highly reproducible junction parameters if one is to achieve a high yield of magnetometers with near optimum performance. Given the relatively wide spread of junction parameters currently achievable, the yield of integrated magnetometers with low noise is likely to be poor. The excellent performance of our multiloop magnetometer was somewhat fortuitous; the junction parameters of our integrated magnetometers, fabricated with nominally the same process, were considerably less favorable.

In most of the multilayer processes reported, $SrTiO_3$ is used as the insulator between the two superconducting layers. However, because of its high dielectric constant, high-frequency resonances were observed for monolithic flux transformer coupled SQUIDs [18,48,49], degrading the SQUID performance. This problem could be ameliorated by the incorporation of a damping resistor [52]. This would also allow one to operate SQUIDs with a large β_L without degrading the transfer function V_Φ [55].

Finally, the magnetic field noise values achieved are in principle adequate for a number of applications, for example, magnetocardiology. However, all the noise measurements reported in this paper were performed in near-zero ambient magnetic field. It has been shown [56] that magnetometers cooled in fields of the order of the earth's magnetic field have considerably higher levels of $1/f$ noise, caused by the thermally activated motion of vortices. One solution to this problem is to operate high-T_c magnetometers in a low ambient magnetic field (say, $\lesssim 10$ μT) to achieve high sensitivity at low frequencies. Instead of expensive mu-metal rooms, field cancellation techniques could perhaps be used. An intriguing alternative [57] is to cool the device in zero field, and then move it into the earth's magnetic field with a "flux dam" (weak link) in the pickup loop to limit the supercurrents induced and thus prevent the entry of flux into the material. More work on this crucial issue of low-frequency noise in nonzero fields is very much in order.

Acknowledgements—We thank D. T. Nemeth for his supporting work in the device fabrication, and L. P. Lee and K. Char for helpful discussions on fabrication issues. We acknowledge the use of the Electronics Research Laboratory of the Electrical Engineering and Computer Department at the University of California, Berkeley, and

are indebted to N. Newman for his invaluable assistance with the X-ray diffractometer. We thank M. Teepe and L. P. Lee for depositing a YBCO film on one of our bicrystal substrates for making SQUIDs. The design and the masks for the multiloop magnetometer were made by S. Knappe, D. Drung and H. Koch, and the sintered YBCO tube was provided by T. W. Button and N. McN. Alford. The AFM and SEM studies were performed by R. E. Thomson and S. Knappe, respectively. This work was supported by the California Competitive Technology Program in collaboration with Conductus, Inc. and by the Director of the Office of Energy Research, Office of Basic Energy Sciences, Materials Sciences Division of the U.S. Department of Energy under Contract no. DE-AC03-76SF00098.

REFERENCES

1. J. Clarke, *NATO ASI Series Superconductive Electronics* (Edited by M. Nisenoff and H. Weinstock) p. 87. Springer, Berlin (1989).
2. R. Gross, P. Chaudhari, M. Kawasaki, M. B. Ketchen and A. Gupta, *Appl. Phys. Lett.* **57**, 727 (1990).
3. G. Friedl, M. Vildic, B. Roas, D. Uhl, F. Bömmel, M. Römheld, B. Hillenbrand, B. Stritzker and G. Daalmans, *Appl. Phys. Lett.* **60**, 3048 (1992).
4. D. Koelle, A. H. Miklich, E. Dantsker, F. Ludwig, D. T. Nemeth, John Clarke, W. Ruby and K. Char, *Appl. Phys. Lett.* **63**, 3630 (1993).
5. J. Z. Sun, W. J. Gallagher, A. C. Callegari, V. Foglietti and R. H. Koch, *Appl. Phys. Lett.* **63**, 1561 (1993).
6. L. P. Lee, J. Longo, V. Vinetskiy and R. Cantor, *Appl. Phys. Lett.* **66**, 1539 (1995).
7. M. Kawasaki, P. Chaudhari, T. H. Newman and A. Gupta, *Appl. Phys. Lett.* **58**, 1555 (1991).
8. D. Grundler, R. Eckart, B. David and O. Dössel, *Appl. Phys. Lett.* **62**, 2134 (1993).
9. K. Hermann, Y. Zhang, M. Mück, J. Schubert, W. Zander and A. I. Braginski, *Supercond. Sci. Technol.* **4**, 453 (1991).
10. D. Koelle, A. H. Miklich, F. Ludwig, E. Dantsker, D. T. Nemeth and John Clarke, *Appl. Phys. Lett.* **63**, 2271 (1993).
11. Y. Zhang, M. Mück, K. Herrmann, J. Schubert, W. Zander, A. I. Braginski and C. Heiden, *IEEE Trans. Appl. Supercond.* **3**, 2465 (1993).
12. Y. Zhang, U. Krüger, R. Kutzner, R. Wördenweber, J. Schubert, W. Zander, M. Strupp, E. Sodtke and A. I. Braginski, *Appl. Phys. Lett.* **65**, 3380 (1994).
13. R. Cantor, L. P. Lee, M. Teepe, V. Vinetskiy and J. Longo, *IEEE Trans. Appl. Supercond.* **5**, 2927 (1995).
14. J. E. Zimmerman, *J. Appl. Phys.* **42**, 4483 (1971).
15. F. Ludwig, E. Dantsker, D. T. Nemeth, D. Koelle, A. H. Miklich, John Clarke, S. Knappe, H. Koch and R. E. Thomson, *Supercond. Sci. Technol.* **7**, 273 (1994).
16. F. Ludwig, D. Koelle, E. Dankster, D. T. Nemeth, A. H. Miklich, John Clarke and R. E. Thomson, *Appl. Phys. Lett.* **66**, 373 (1995).
17. F. Ludwig, E. Dantsker, R. Kleiner, D. Koelle, John Clarke, S. Knappe, D. Drung, H. Koch, Neil McN. Alford and T. W. Button, *Appl. Phys. Lett.* **66**, 1418 (1995).
18. F. Ludwig, E. Dantsker, D. Koelle, R. Kleiner, A. H. Miklich, D. T. Nemeth, John Clarke, D. Drung, S. Knappe and H. Koch, *IEEE Trans. Appl. Supercond.* **5**, 2919 (1995).
19. E. Dantsker, F. Ludwig, R. Kleiner, John Clarke, M. Teepe, L. P. Lee, Neil McN. Alford and T. Button, *Appl. Phys. Lett.* **66**, 725 (1995).
20. D. D. Tesche and J. Clarke, *J. Low Temp. Phys.* **29**, 301 (1977).
21. K. Enpuku, Y. Shimomura and T. Kisu, *J. Appl. Phys.* **73**, 7929 (1993).
22. M. N. Keene, J. S. Satchell, S. W. Goodyear, R. G. Humphreys, J. A. Edwards, N. G. Chew and K. Lander, *IEEE Trans. Appl. Supercond.* **5**, 2923 (1995).
23. R. H. Koch, *Fourth International Superconductive Electronics Conference*, Boulder, CO (1993) (unpublished).
24. R. Kleiner (unpublished).
25. M. B. Ketchen, W. J. Gallagher, A. W. Kleinsasser, S. Murphy, and J. R. Clem, in *SQUID '85* (Edited by H. D. Hahlbohm and H. Lübbig), p. 865. Walter de Gruyter, Berlin (1985).
26. D. Drung, private communication.
27. J. M. Jaycox and M. B. Ketchen, *IEEE Trans. Magn.* **MAG-17**, 400 (1981).
28. D. Drung, S. Knappe and H. Koch, *J. Appl. Phys.* **77**, 4088 (1995).
29. J. J. Kingston, F. C. Wellstood, Ph. Lerch, A. H. Miklich and J. Clarke, *Appl. Phys. Lett.* **56**, 189 (1990).
30. B. Roas, G. Friedl, L. Bär, F. Bömmel, G. Daalmans and L. Schultz, *IEEE Trans. Appl. Supercond.* **3**, 2442 (1993).
31. J. J. Kingston, F. C. Wellstood, D. Quan, and John Clarke, *IEEE Trans. Magn.* **MAG-27**, 974 (1991).
32. B. Oh, R. H. Koch, W. J. Gallagher, R. P. Robertazzi and W. Eidelloth, *Appl. Phys. Lett.* **59**, 123 (1991); W. Eidelloth, W. J. Gallagher, R. H. Koch and B. Oh, *Appl. Phys. Lett.* **59**, 1257 (1991).
33. L. P. Lee, K. Char, M. S. Colclough and G. Zaharchuk, *Appl. Phys. Lett.* **59**, 3051 (1991).
34. M. S. Dilorio, S. Yoshizumi, M. Maung, J. Zhang and B. Power, *IEEE Trans. Appl. Supercond.* **3**, 2011 (1993).
35. A. H. Miklich, J. J. Kingston, F. C. Wellstood, J. Clarke, M. S. Colclough, K. Char and G. Zaharchuk, *Appl. Phys. Lett.* **59**, 988 (1991).
36. M. N. Keene, S. W. Goodyear, N. G. Chew, R. G. Humphreys, J. S. Satchell, J. A. Edwards and K. Lander, *Appl. Phys. Lett.* **64**, 366 (1994).
37. B. R. David, D. Grundler, R. Eckart, K. Fanghänel, J. P. Krumme, V. Doormann and O. Dössel, *Supercond. Sci. Technol.* **7**, 287 (1994).
38. F. C. Wellstood, J. J. Kingston and J. Clarke, *Appl. Phys. Rev.* **75**, 683 (1994).
39. A. H. Miklich, D. Koelle, E. Dantsker, D. T. Nemeth, J. J. Kingston, R. F. Kromann and J. Clarke, *IEEE Trans. Appl. Supercond.* **3**, 2434 (1993).
40. R. H. Koch, J. Clarke, W. M. Goubau, J. M. Martinis, C. M. Pegrum and D. J. Van Harlingen, *J. Low Temp. Phys.* **51**, 207 (1983).
41. M. J. Farrari, M. Johnson, F. C. Wellstood, J. Clarke, P. A. Rosenthal, R. H. Hammond and M. R. Beasley, *Appl. Phys. Lett.* **53**, 695 (1988).

42. M. J. Ferrari, J. J. Kingston, F. C. Wellstood and John Clarke, *Appl. Phys. Lett.* **58**, 1106 (1991); F. C. Wellstood, J. J. Kingston, M. J. Ferrari and John Clarke, *IEEE Trans. Magn.* **MAG-27**, 2569 (1991).
43. N. Missert, T. E. Harvey, R. H. Ono and C. D. Reintsma, *Appl. Phys. Lett.* **63**, 1690 (1993).
44. R. H. Koch, private communication.
45. M. Strikovski, J. Schubert, G. Ockenfluß, R. Wördenweber, U. Gassig and W. Zander, *Proceedings of the European Conference on Applied Superconductivity (EUCAS)* (Edited by H. C. Freyhardt), p. 651. DGM Informationsgesellschaft mbH, Oberursel (1993).
46. T. W. Button, N. McN. Alford, F. Wellhofer, T. C. Shields, F. S. Abell and M. Day, *IEEE Trans. Magn.* **MAG-27**, 1434 (1991).
47. R. Kromann, J. J. Kingston, A. H. Miklich, L. T. Sagdahl and John Clarke, *Appl. Phys. Lett.* **63**, 559 (1993).
48. B. David, D. Grundler, J.-P. Krumme and O. Dössel, *IEEE Trans. Appl. Supercond.* **5**, 2935 (1995).
49. J. W. M. Hilgenkamp, G. C. S. Brons, J. G. Soldevilla, R. P. Isselsteijn, J. Flokstra and H. Rogalla, *Appl. Phys. Lett.* **64**, 3497 (1994).
50. M. B. Ketchen, *IEEE Trans. Magn.* **MAG-27**, 2916 (1991).
51. D. Grundler, B. David and O. Dössel, *J. Appl. Phys.* **77**, 5273(1995).
52. V. Foglietti, W. J. Gallagher, M. B. Ketchen, A. W. Kleinsasser, R. H. Koch and R. L. Sandstrom, *Appl. Phys. Lett.* **55**, 1451 (1989).
53. O. Dössel, B. David, R. Eckart, D. Grundler and S. Kreff, *Proceedings of the 2nd Workshop on HTS Applications and New Materials*, Twente, The Netherlands, p. 124 (1995).
54. See, for example, *Proceedings of Applied Superconductivity Conference*, Boston, 1994 in *IEEE Trans. Appl. Supercond.* **5** (1995).
55. K. Enpuku, K. Sueoka, K. Yoshida and F. Irie, *J. Appl. Phys.* **57**, 1691 (1985).
56. A. H. Miklich, D. Koelle, T. J. Shaw, F. Ludwig, D. T. Nemeth, E. Dantsker, John Clarke, Neil McN. Alford, T. W. Button and M. S. Colclough, *Appl. Phys. Lett.* **64**, 3494 (1994).
57. J. Z. Sun, L. S. Yu-Jahnes, V. Foglietti, R. H. Koch and W. J. Gallagher, *IEEE Trans. Appl. Supercond.* **5**, 2107 (1995); R. H. Koch, J. Z. Sun, V. Foglietti and W. J. Gallagher, *Appl. Phys. Lett.* **67**, 704 (1995).